

UNCLASSIFIED

SECURITY CLASSIFICATION OF THIS PAGE

| REPORT DOCUMENTATION PAGE  |   |   |  |   |
|--|---|---|--|---|
| 1a. REPORT SECURITY CLASSIFICATION<br><b>Unclassified</b>  |   | 1b. RESTRICTIVE MARKINGS<br><b>None</b>   |  |   |
| 2a. SECURITY CLASSIFICATION AUTHORITY  |   | 3. DISTRIBUTION/AVAILABILITY OF REPORT<br><br><b>Approved for public release; distribution is unlimited.</b>                      |  |   |
| 2b. DECLASSIFICATION/DOWNGRADING SCHEDULE  |   |   |  |   |
| 4. PERFORMING ORGANIZATION REPORT NUMBER(S)<br><br><b>NORDA Report 161</b>   |   | 5. MONITORING ORGANIZATION REPORT NUMBER(S)<br><br><b>NORDA Report 161</b>  |  |   |
| 6. NAME OF PERFORMING ORGANIZATION<br><br><b>Naval Ocean Research and Development Activity</b>   |   | 7a. NAME OF MONITORING ORGANIZATION<br><br><b>Naval Ocean Research and Development Activity</b>                                   |  |   |
| 6c. ADDRESS (City, State, and ZIP Code)<br><br><b>Ocean Acoustics and Technology Directorate<br/>NSTL, Mississippi 39529-5004</b>  |   | 7b. ADDRESS (City, State, and ZIP Code)<br><br><b>Ocean Acoustics and Technology Directorate<br/>NSTL, Mississippi 39529-5004</b> |  |   |
| 8a. NAME OF FUNDING/SPONSORING ORGANIZATION<br><br><b>Space and Naval Warfare<br/>Systems Command</b>  | 8b. OFFICE SYMBOL<br>(If applicable)<br><br><b>SPAWAR</b> | 9. PROCUREMENT INSTRUMENT IDENTIFICATION NUMBER   |  |   |
| 8c. ADDRESS (City, State, and ZIP Code)<br><br><b>Washington, D.C. 20380</b>   |   | 10. SOURCE OF FUNDING NOS.  |  |   |
|  |   | PROGRAM<br>ELEMENT NO.<br><b>62435N</b>   | PROJECT<br>NO.   | TASK<br>NO.                               |
|  |   |   | WORK UNIT<br>NO.   |   |
| 11. TITLE (Include Security Classification)<br><b>Geoacoustic Models of the Hudson Canyon Area</b>   |   |   |  |   |
| 12. PERSONAL AUTHOR(S)<br><b>C. E. Sellinger and D. L. Lavoie</b>  |   |   |  |   |
| 13a. TYPE OF REPORT<br><br><b>Final</b>  | 13b. TIME COVERED<br>From _____ To _____                  | 14. DATE OF REPORT (Yr., Mo., Day)<br><br><b>December 1986</b>  |  | 15. PAGE COUNT<br><br><b>11</b>           |
| 16. SUPPLEMENTARY NOTATION   |   |   |  |   |
| 17. COSATI CODES   |   |   | 18. SUBJECT TERMS (Continue on reverse if necessary and identify by block number)<br><br><b>geoacoustic models, sediment type, stratigraphy, Hudson Canyon</b> |   |
| FIELD  | GROUP   | SUB. GR.  |  |   |
|  |   |   |  |   |
|  |   |   |  |   |
| 19. ABSTRACT (Continue on reverse if necessary and identify by block number)<br><br>To better understand the interaction of sound wave propagation with the sea floor, three geographic sites were selected for modeling. These sites compose a region that begins at a water depth of 75 m and continues to approximately 5050 m. Surficial sediments range from a sand-silt-clay fluvial deposit on the shelf to a "red clay" and a clay-sized calcareous ooze. Structural features, such as the Hudson Canyon area, the Hatteras Outer Ridge, a lower Cretaceous carbonate reef, and a deep structural basin, play a strong historical role in shaping the sediment distribution and topography in this region. Several prominent horizons, A <sup>U</sup> , A*, and $\beta$ are identified using graphically descriptive profiles. Three geoacoustic models of each site were developed using Hamilton's techniques. These models provide depth to horizons, compressional wave velocities, shear wave velocities, densities, and attenuation of the individual sediment type. |   |   |  |   |
| 20. DISTRIBUTION/AVAILABILITY OF ABSTRACT<br><br>UNCLASSIFIED/UNLIMITED <input type="checkbox"/> SAME AS RPT. <input checked="" type="checkbox"/> DTIC USERS <input type="checkbox"/>  |   | 21. ABSTRACT SECURITY CLASSIFICATION<br><br><b>Unclassified</b>   |  |   |
| 22a. NAME OF RESPONSIBLE INDIVIDUAL<br><br><b>C. E. Sellinger</b>  |   | 22b. TELEPHONE NUMBER (Include Area Code)<br><br><b>(601) 688-5784</b>  |  | 22c. OFFICE SYMBOL<br><br><b>Code 222</b> |



# Naval Ocean Research and Development Activity

January 1987

(NORDA - Report-161)

## Geoacoustic Models of the Hudson Canyon Area

LIBRARY  
RESEARCH REPORTS DIVISION  
NAVAL POSTGRADUATE SCHOOL  
MONTEREY, CALIFORNIA 93940

C. E. Sellinger

Numerical Modeling Division

Ocean Acoustics and Technology Directorate

D. L. Lavoie

Ocean Science Directorate

Seafloor Geosciences Division

# Foreword

---

This report summarizes the geology of three specific sites in the vicinity of the Hudson Canyon. Each site is accompanied by a geoacoustic model that outlines the compressional and shear wave velocities, as well as compressional wave attenuation and density of sediment with depth. These models will aid in the prediction of critical acoustic parameters.

A handwritten signature in black ink, appearing to read 'A C Esau'.

**A. C. Esau, Captain, USN  
Commanding Officer, NORDA**

# Executive summary

---

To better understand the interaction of sound wave propagation with the sea floor, three geographic sites were selected for modeling. These sites compose a region that begins at a water depth of 75 m and continues to approximately 5050 m. Surficial sediments range from a sand-silt-clay fluvial deposit on the shelf to a "red clay" and a clay-sized calcareous ooze. Structural features, such as the Hudson Canyon area, the Hatteras Outer Ridge, a lower Cretaceous carbonate reef, and a deep structural basin, play a strong historical role in shaping the sediment distribution and topography in this region. Several prominent horizons,  $A^u$ ,  $A^*$ , and  $\beta$  are identified using graphically descriptive profiles. Three geoacoustic models of each site were developed using Hamilton's techniques. These models provide depth to horizons, compressional wave velocities, shear wave velocities, densities, and attenuation of the individual sediment type.

# Acknowledgments

---

This effort is sponsored by the Space and Naval Warfare Systems Command, and is a part of the Bottom Interaction Program. Dr. J. Alan Ballard and Ms. Muriel Grim, Marine Geophysical Branch, NORDA Seafloor Geosciences Division, are acknowledged for their thorough technical edit of this report. Ms. Renee Edman and Mr. Joseph Pearson of NORDA's Technical Information Branch provided graphics assistance. Finally, Mr. Joseph Soileau of NORDA Code 241 was instrumental in gathering the statistics on physical oceanographic parameters. This project was funded by the Office of Naval Technology under program element 62435.

# Contents

---

|                            |   |
|----------------------------|---|
| <b>Introduction</b>        | 1 |
| <b>Setting</b>             | 1 |
| <b>Acoustic horizons</b>   | 1 |
| <b>Surficial sediments</b> | 2 |
| <b>Stratigraphy</b>        | 3 |
| Site A                     | 3 |
| Site B                     | 3 |
| Site C                     | 3 |
| <b>Geoacoustic models</b>  | 6 |
| <b>Summary</b>             | 6 |
| <b>Bibliography</b>        | 5 |



# Geoacoustic Models of the Hudson Canyon Area

---

## Introduction

This report provides general geological/geophysical data and geoacoustic models in the Hudson Canyon area. A geoacoustic model is defined as a numerical representation of the real sea floor with emphasis on measured, extrapolated, predicted values of those properties important in underwater acoustics and those aspects of geophysics involving sound transmission interaction. Three sites were chosen in the Outer Hudson Canyon area for modeling. Surface and stratigraphic data were gathered with emphasis on sediment type, grain size, acoustic reflectors, sound speed, water depth, and water velocities. With these data in hand, Edwin Hamilton's (1980) sea-floor modeling techniques were used to produce geoacoustic models. These models, in turn, were used in support of the Fiscal Year 1985 Broadband Acoustic Experiment managed by Dr. Peter Herstein, Naval Underwater Systems Center (NUSC), and Mr. Jack Shooter, Applied Research Laboratories/University of Texas (ARL/UT).

## Setting

The study area (Fig. 1) includes portions of the continental shelf, slope, and rise on the eastern United States coast south of Long Island. This area forms a triangle situated between sites A ( $35^{\circ}30'N$  and  $71^{\circ}29'W$ ), B ( $40^{\circ}29'N$  and  $71^{\circ}53'W$ ), and C ( $36^{\circ}00'N$  and  $67^{\circ}00'W$ ). The slope ratio on the slope is 1:53 and the ratio on the rise is 1:239. Bottom topography within the study area is smooth on the shelf and rough on the slope, especially in the vicinity of the Hudson Canyon.

The Hudson Canyon occupies a major portion of the study area. Sediments in the canyon consist of reworked Pleistocene sands and gravels (Keller et al., 1979). The canyon axis, through which sediment is funneled from the shelf to the rise, trends southeast. Just beyond the canyon axis, buried beneath the present-day surface, lies the Hatteras Outer Ridge. The ridge covers the southeast sub-bottom portion of the study area (Fig. 2). Formed during the late Pliocene, the Hatteras Outer Ridge is a large drift deposit of fine-grained contourite sediments approximately 500 m thick. The deposit was formed by the interaction of the Western Boundary Undercurrent and the Gulf Stream (Tucholke and Laine, 1982).

## Acoustic horizons

An acoustic horizon is the surface separating two sediment or rock layers of different acoustic impedance, where this surface is associated with a reflection that can be carried over a large area (Sheriff, 1984). In this area are four major horizons:  $A^u$ ,  $A^*$ ,  $\beta$ , and X (Benson et al., 1978).

Three profiles depicting the relationship of the acoustic horizons are provided (Figs. 4, 5, and 6). These profiles are scaled to the acoustic horizon using two-way travel time. The authors wish to show these increments, since this is measured data, whereas the depth in meters from Tables I, II, and III are calculated.

The youngest and shallowest horizon, X, is a mid-Miocene reflecting zone (Tucholke and Laine, 1982). It displays small-scale relief and is present at site A only (Fig. 3). This reflector caps the crest of the Hatteras Outer Ridge in this area (Ewing and Rabinowitz, 1984). Horizon X is an irregular interface that in some places truncates the older and deeper reflector  $A^u$  (Fig. 4).

Below horizon X in most portions of the study area is the older horizon  $A^u$ , which represents a regional unconformity, the result of a period of erosion by boundary undercurrents. From early to middle Oligocene, the continental rise of the U.S. was deeply eroded by the southwest-flowing Western Boundary Undercurrent, which truncated beds ranging in age from early Cretaceous to middle Eocene. This horizon,  $A^u$ , mapped at Deep Sea Drilling Project (DSDP) Site 388, is located approximately 490 m below the sediment-water interface. At site A, horizon  $A^u$  is overlain by a terrigenous turbidite, and at sites B and C it is bounded above by fluvial sandy-silt and calcareous ooze, respectively.

Still older, horizon  $A^*$  is a prominent reflector found below horizon  $A^u$  throughout much of the area (Fig. 3). Horizon  $A^*$  represents the contact between upper Cretaceous variegated clays and the underlying Cretaceous black clays. Horizon  $A^*$  has been identified at a depth of 700 m at DSDP Site 388. West of the Bermuda Rise, horizon  $A^*$  is widespread but merges with and is truncated by horizon  $A^u$  in the east as it approaches the continental shelf, and truncates horizon  $\beta$  near the Kelvin Seamounts.

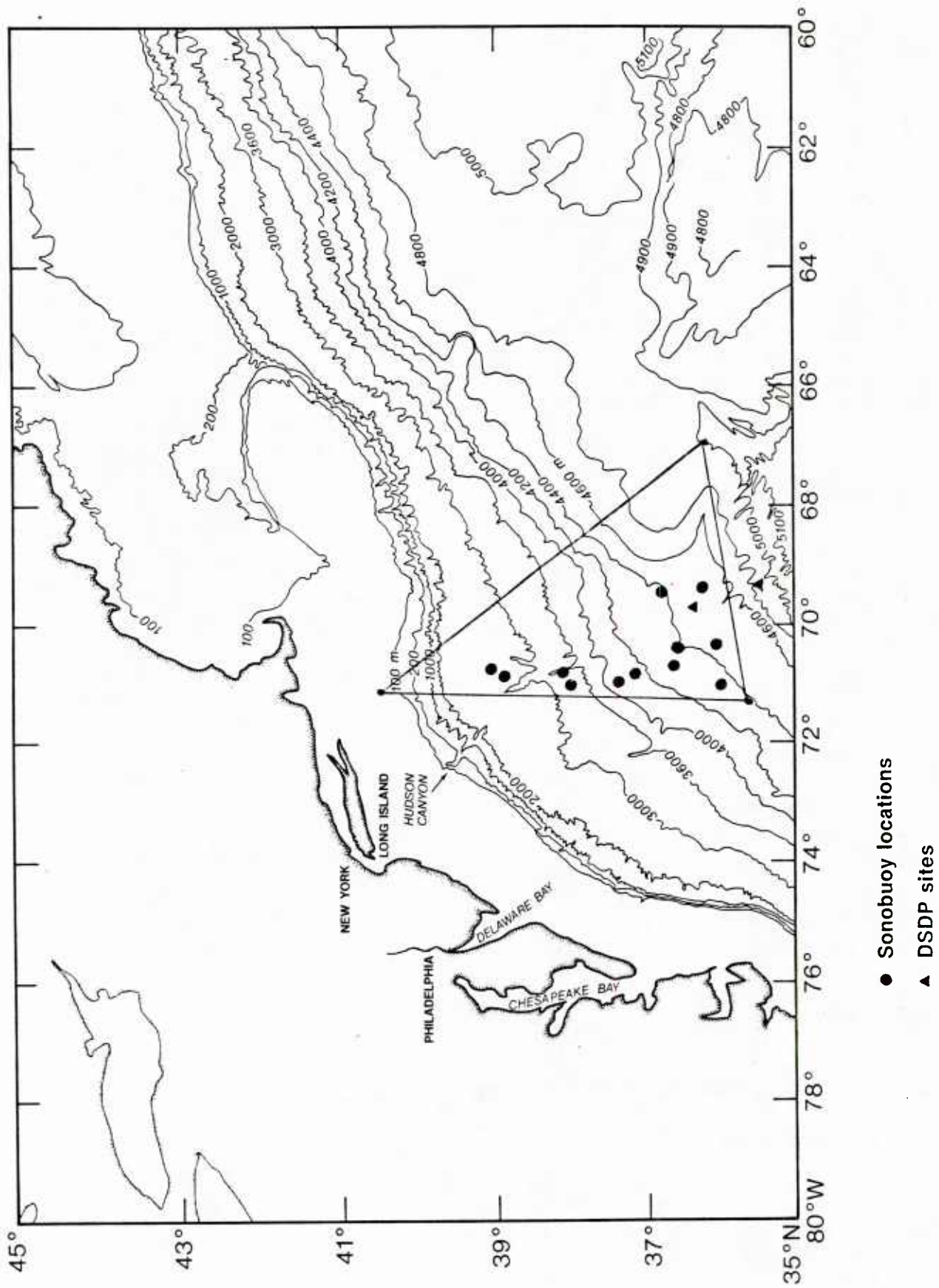


Figure 1. Site map with sonobuoy and DSDP drillhole locations.



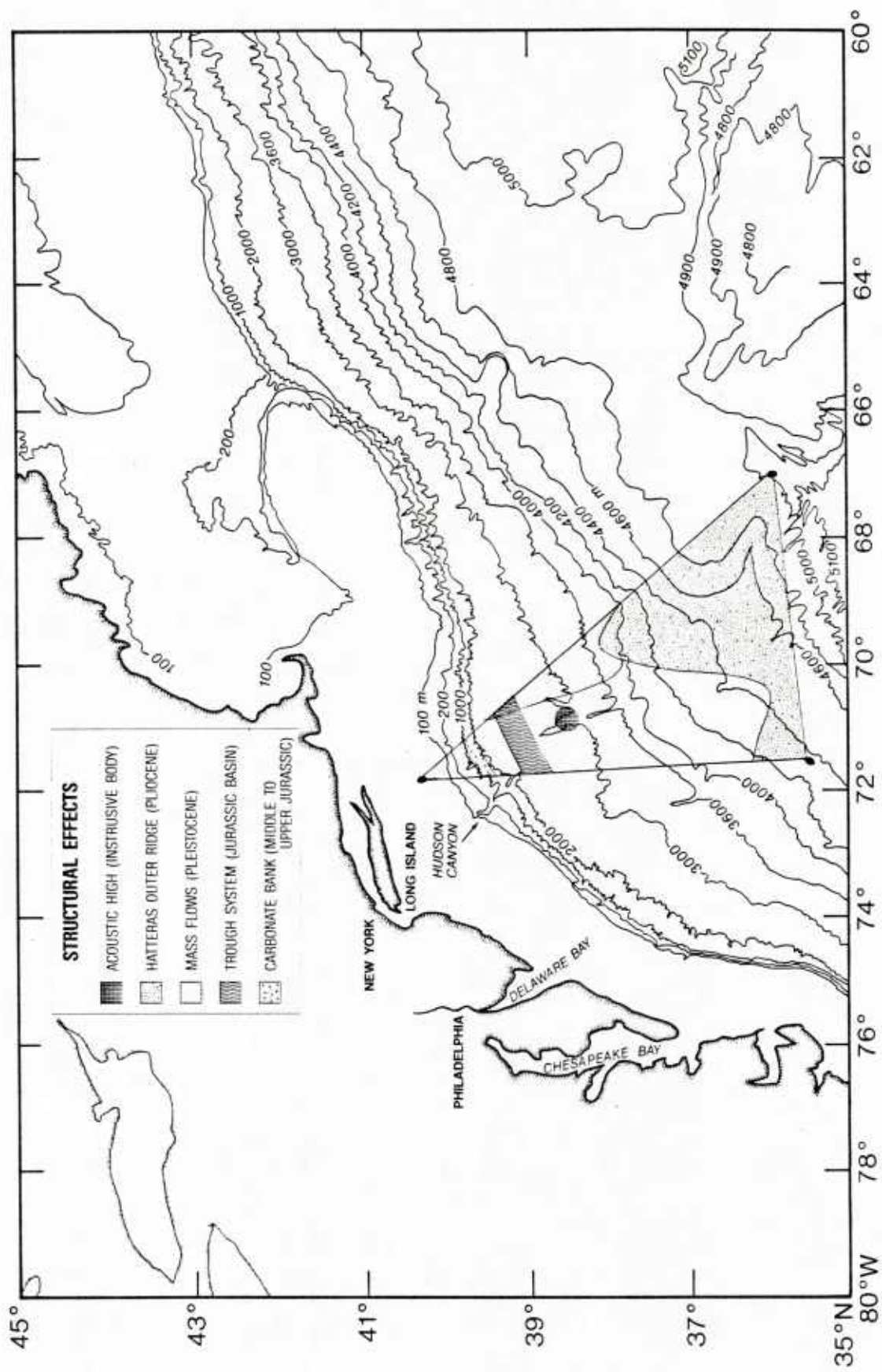


Figure 2. Structural features map.

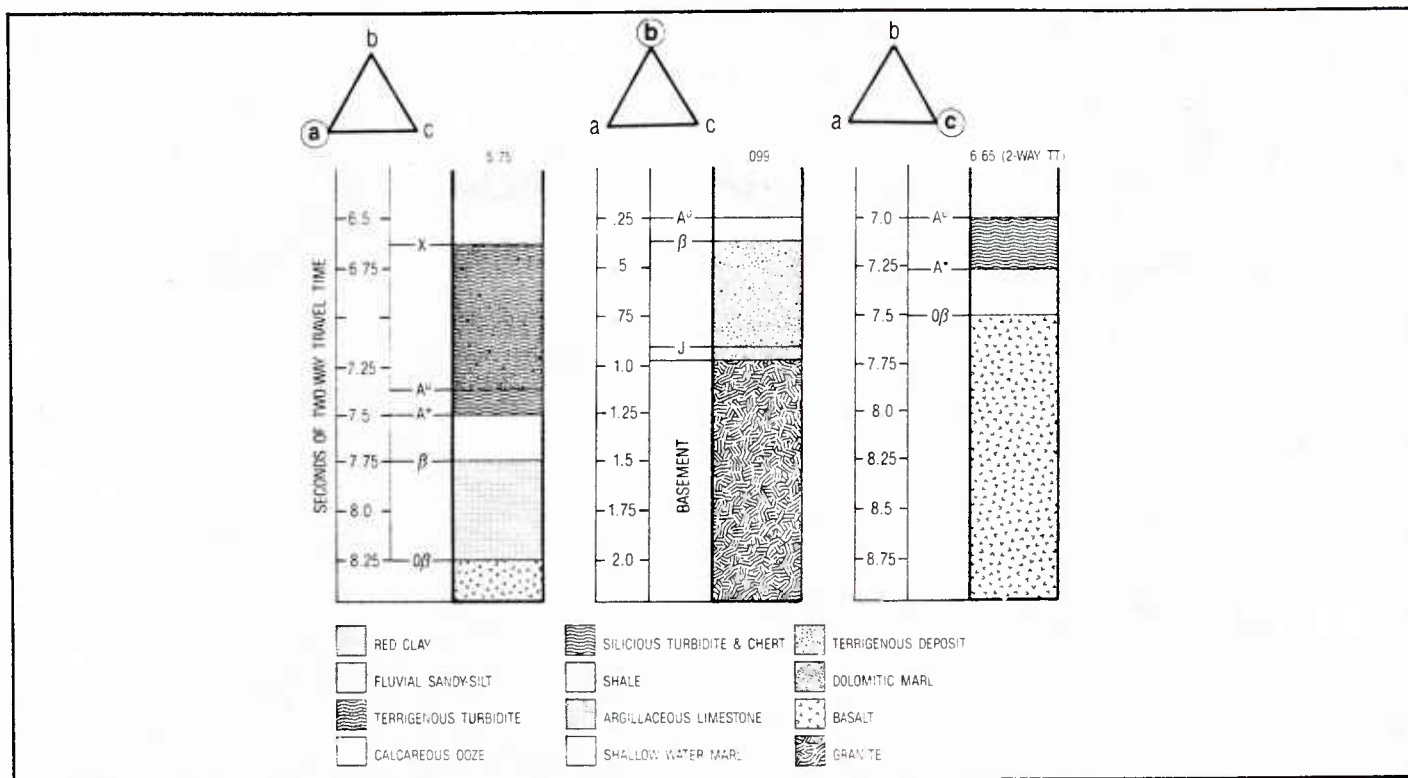


Figure 3. Stratigraphic sequence chart.

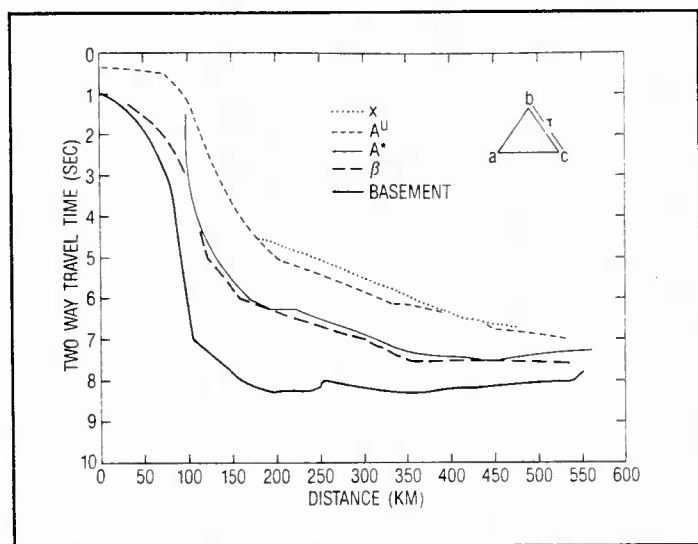


Figure 4. Acoustic horizon profile 2.

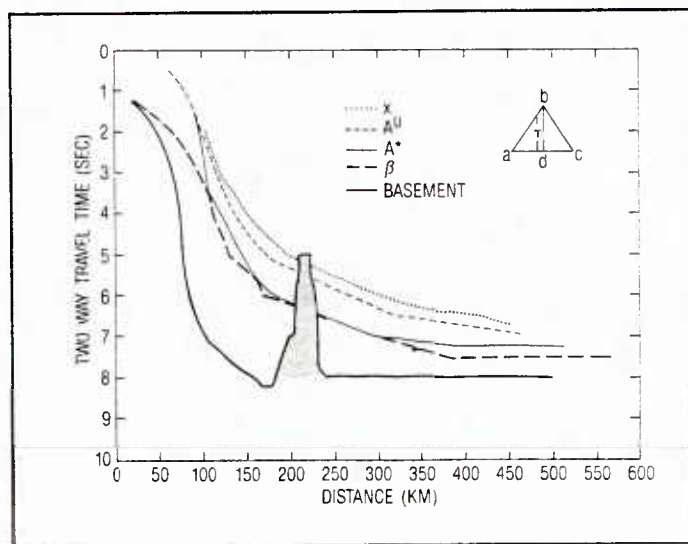


Figure 5. Acoustic horizon profile 1.

Horizon  $\beta$  is usually associated with a Neocomian-Tithonian white and gray limestone (Benson et al., 1978). Near DSDP Site 388 and Site 105 the gray limestone overlies Kimmeridgian-Oxfordian red, clayey limestone, which in turn overlies the basaltic basement. Actual oceanic basaltic basement, identified on seismic records by Ewing and Rabinowitz (1984), is present throughout most of the area from midway below the continental slope seaward and includes sites A and C.

A weak acoustic reflector in this area, J, exists at site B and extends southwestward to near site A. Below this

Jurassic reflector (Fig. 3) is a dolomitic deposit that separates the above terrigenous sediment from the granitic basement (Ewing and Rabinowitz, 1984).

## Surficial Sediments

Surficial sediments in the study area are composed of calcareous oozes and "red-colored clays" on the slope and rise (Fig. 3) and fluvial marine sediments on the shelf (Bennett et al., 1980).

Outer Hudson Canyon sand, silt, and clay sediments are highly variable in texture and are slightly coarser in overall

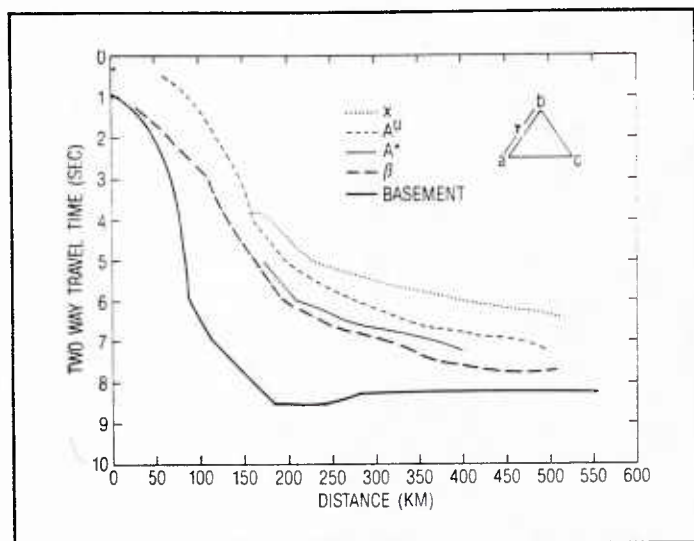


Figure 6. Acoustic horizon profile 3.

grain size than upper rise deposits. Canyon valley axis sediments vary from silty-clay to gravel often in identifiable turbidite sequences. Sediment on the canyon walls and levees often display fine, silty banding in a silty-clay matrix (Bennett et al., 1980). Sedimentation rates in this portion of the North Atlantic have been high since early Miocene (Hollister et al., 1972). Turbidity currents, turbulent suspensions of water and sediment, and mass sediment flows, without the addition of water to the original sediment, have been funneled through Hudson Canyon and have built a large fan.

Turbidite deposits are noted throughout the area, mainly below reflector X (Fig. 3). At least 40% of the continental rise of eastern North America from the New England Seamounts to the Blake-Bahama Outer Ridge are covered with a veneer of mass flow deposits (Embley, 1980).

Scientists from DSDP Leg 106 reported that during Eocene-early Miocene, sediment accumulation was 0.2 cm/1000 yr. During the Miocene-Pliocene interval the sedimentation rate reached 4.3 cm/1000 yr. By the Pleistocene, the sedimentation rate had increased to 20 cm/1000 yr, exceeding all rates previously determined for Pleistocene accumulation in the major ocean basins.

## Stratigraphy

One of the primary goals of this project was to define the layering structure of the subsurface sediments within the study area. Much of the surficial sediment data was based on Hydroplastic short cores collected and analyzed for the National Oceanic and Atmospheric Administration's Marine Geotechnical Program. Only two DSDP sites (holes 106 and 388) are near the area of interest (Fig. 1). Much of the stratigraphy, therefore, was determined from seismic reflection profiles with depths to various horizons mapped and correlated with DSDP data. Thus, the sediment structure can best be described by using the acoustic horizons as boundaries.

## Site A

"Red clay" is the dominant surface sediment at Site A (Bennett et al., 1980). The term red clay is used to denote the iron-rich red color and does not infer a generic deep-sea red clay. This sequence extends from the surface to a depth of 617 m and is bounded by reflector X (Fig. 3). The red clay is a fine-grained inorganic sediment material that varies in texture and mineralogy, and consists of clay minerals and admixtures of carbonate debris. This clay is widespread in the southwestern portion of the area.

Below reflector X is a terrigenous turbidite layer extending another 579 m (Table I). The average interval velocity is 1.8 km/sec. This silty-clay sequence forms the Hatteras Outer Ridge and trends northeast through the study area.

Beneath horizon A<sup>u</sup> is a thin layer of siliceous turbidite approximately 99 m thick, with stringers of chert. This layer has a compressional wave velocity of 2.0 km/sec (Table I) and appears to contain a completely silicified layer near the bottom just above horizon A\* (Hollister et al., 1972).

A carbonaceous shale (Benson et al., 1978) underlies horizon A\* for 192 m and has an interval velocity of 3.5 km/sec. At a calculated 1487 m, horizon β caps a limestone sequence. This sequence has a thickness of 398 m and an interval velocity of 3.5 km/sec (Table I). Basement is oceanic basalt.

## Site B

Surficial sediments of this shelf site are fluvial marine sediments, sands with patches of Pleistocene clays, to a calculated depth of 600 m. At water depths of 900 to 1000 m, the upper continental slope is characterized by several centimeters of top sand overlying the clayey silts and silty clays. The lower boundary of this unit is delimited by A<sup>u</sup> (Table II). Since the buried Hatteras Outer Ridge does not extend this far, horizon X is missing from this sequence. The sediment between A<sup>u</sup> and β is a shallow water marl with a thickness of 100 m and an interval velocity of 2.02 km/sec. Between horizon β and horizon J are 600 m of a sand-silt-clay terrigenous deposit. Below J is a dolomitic marl layer approximately 100 m thick with an interval velocity of 3.1 km/sec. Below this dense marl is granitic basement with a calculated velocity of 5.5 km/sec.

## Site C

At site C, in the southeastern tip of the study area, surficial sediments are primarily calcareous oozes. Such deposits are at least 30% calcium carbonate, usually in the form of skeletal material (Bennett et al., 1980). Site C differs from site A in that it is capped with a calcareous ooze and horizon X is missing. Sediment between A<sup>u</sup> and A\* is a siliceous turbidite with chert, the same as at site A. This layer has a thickness of 173 m, an average density of 1.8 g/cm<sup>3</sup>, and an interval velocity of 2.02 km/sec (Table III). Beneath A\* is a carbonaceous shale, with a thickness of approximately 194 m and an averaged calculated velocity of 2.3 km/sec. The horizon β and the limestone sequence



have disappeared; otherwise, the sediment sequence is the same as at site A. Throughout the area the basaltic basement is fairly rough; Figure 5 shows a mafic intrusion.

## Geoacoustic models

The seismic and stratigraphic data used to calculate these geoacoustic models were interpreted from actual data locations (Fig. 1). Because of the nature of the input data, these models represent an educated guess of the acoustic parameters at the individual sites.

This interpreted data was used to calculate the various values in Tables I, II and III. Edwin Hamilton's (1980) modeling techniques were used for the upper unconsolidated layers, and previously measured data was used for assumed lithified material.

Sonobuoy data provided the interval velocities between reflectors previously discussed. In addition, DSDP holes 388 and 106, as well as an industrial well, provided measured compressional velocity data (Fig. 1). From these data, the geological description of the area, and compiled data on average sediment properties, geoacoustic models for sites A, B, and C were developed. These models were constructed using the classical Hamilton Technique (Hamilton, 1980).

The sediment type, grain size, and density were determined from core data and published literature. Water column velocities and depths were obtained from a NORDA data bank (Soileau, 1985). Sound speed, interval velocities, subsurface sediments, and acoustic reflector information were obtained from Ewing and Rabinowitz (1984). Surficial sediment data were taken from Bennett et al. (1980).

## Summary

Several geologic events determined the layering structure in this study area. An erosional unconformity, A<sup>u</sup> was formed by the Western Boundary Undercurrent. Turbidity currents and mass sediment flows were large contributors to sediment deposition. Since this broadband experiment involves a wide frequency range, these episodes of deposition and erosion were researched from the sediment surface interface into the oceanic basement. The resulting calculated velocities for the top layers agree well with nearby sonobuoy data. However, as the sediment depth increases, assumptions such as layer consolidation lead to less-reliable-appearing calculated values and to greater reliance on the use of measured values.

## Bibliography

- Bennett, R. H., G. L. Freeland, D. N. Lambert, W. B. Sawyer, G. H. and Keller (1980). Geotechnical properties of surficial sediments in a mega-corridor: U.S Atlantic Continental Slope, Rise, and Deep-Sea Basin. *Marine Geology* 38, 23-50.
- Benson, W. E. et al. (1978). *Initial Reports of the Deep Sea Drilling Project*. U.S. Government Printing Office, Washington, D.C., v. 44, pp. 5-67.
- Dobrin, M. B. (1976). *Introduction to Geophysical Prospecting*. McGraw-Hill, pp. 48-50.
- Embley, R. W. (1980). The role of mass transport in distribution and character of deep ocean sediments with special reference to the North Atlantic. *J. Mar. Geol.* 38, 23-50.
- Ewing, J. E. and P. D. Rabinowitz (1984). *Ocean Margin Drilling Program Regional Atlas Series (No. 4)*. Marine Science International.
- Hamilton, E. L. (1980). Geoacoustic modeling in the sea floor. *J. Acoust. Soc. Am.* 68(5).
- Hollister, C. D. et al. (1972). *Initial Reports of the Deep Sea Drilling Project*. U. S. Government Printing Office, v. 11, pp. 313-366.
- Keller, G. H., D. N. Lambert, and R. H. Bennett (1979). *Geotechnical Properties of Continental Slope Deposits--Cape Hatteras to Hydrographer Canyon*. SEPM Special Pub. No. 27, pp. 131-151.
- Klitgord, K. D. and J. C. Behrendt (1978). *Basin Structure of the U.S. Atlantic Margin*. AAPG Memoir No. 29.
- McGregor, B. A. (1978). *Seismic Reflection Profiles of the United States East Coast Continental Margin*. National Oceanic and Atmospheric Administration, Report ERL 398-AOML 28.
- Osner, R. K. (1969). *Bottom Environmental Oceanographic Data Report, Hudson Canyon Area*. Naval Oceanographic Officer, NSTL, Mississippi, Report 69-8.
- Sheridan, R. E., J. A. Grow, J. C. Behrendt, and K. C. Beyer (1979). Seismic refraction study of the continental edge off the eastern United States. *Tectonophysics* 59, 1-26.
- Sheriff, R. E. (1984). *Encyclopedic Dictionary of Exploration Geophysics*. Library of Congress, Washington, D.C.
- Tucholke, B. E. and E. P. Laine (1982). Neogene and quaternary development of the lower continental rise off the central U.S. East Coast. *Am. Assoc. Petrol. Geol.* 295-305.

Table I. Geoacoustic model of site A.

| Sediment Type   | Depth (km) | $V_p$ (km/sec) | $V_p(l)$ (km/sec) | $V_s$ (km/sec) | $K_p$ (dB/m/kHz) | $\rho$ (g/cm <sup>3</sup> ) |
|---|------------|----------------|-------------------|----------------|------------------|-----------------------------|
| Water   | 4.350      | 1.530          |                   |                |                  |                             |
| Clay<br>X   | 0.000      | 1.504          | 1.74              | 0.346          | 0.030            | 1.5                         |
|   | 0.100      | 1.627          |                   | 0.365          | 0.088            | 1.7                         |
|   | 0.200      | 1.737          |                   | 0.436          | 0.118            | 1.8                         |
|   | 0.300      | 1.835          |                   | 0.489          | 0.131            | 1.9                         |
|   | 0.400      | 1.923          |                   | 0.545          | 0.133            | 2.0                         |
|   | 0.500      | 2.003          |                   | 0.601          | 0.146            | 2.1                         |
|   | 0.617      | 2.087          |                   | 0.667          | 0.131            | 2.2                         |
| Terrigenous<br>Turbidite<br>A <sup>u</sup>            | 0.700      | 2.154          | 1.84              | 0.718          | 0.120            | 2.3                         |
|   | 0.800      | 2.217          |                   | 0.814          | 0.094            | 2.3                         |
|   | 0.900      | 2.277          |                   | 0.814          | 0.094            | 2.4                         |
|   | 1.000      | 2.336          |                   | 0.860          | 0.082            | 2.5                         |
|   | 1.100      | 2.396          |                   | 0.907          |                  | 2.5                         |
| Siliceous<br>Turbidite<br>and Chert<br>A <sup>*</sup> | 1.200      | 2.183          | 2.0               | 0.741          |                  | 2.3                         |
|   | 1.250      | 2.194          |                   | 0.749          |                  | 2.3                         |
|   | 1.275      | 2.199          |                   | 0.753          |                  | 2.3                         |
|   | 1.295      | 2.203          |                   | 0.756          |                  | 2.3                         |
| Carbonaceous<br>Shale<br>$\beta$                      | 1.300      | 3.131          | 3.52              | 1.480          |                  | 2.3                         |
|   | 1.350      | 3.167          |                   | 1.508          |                  |                             |
|   | 1.400      | 3.201          |                   | 1.535          |                  |                             |
|   | 1.487      | 3.256          |                   | 1.578          |                  |                             |
| Argillaceous<br>Limestone                             | 1.500      | 3.500*         |                   | 1.650*         |                  | 2.58**                      |
|   | 1.885      |                |                   |                |                  |                             |
| Oceanic<br>basement<br>(basalt)                       |            | 5.300**        |                   | 2.680**        | 0.02**           | 2.7**                       |

Notes: The bottom water velocity was taken from Soileau's (1985) NORDA data base. At this site it was 1527.65 m/sec at a depth of 4350. Compressional wave velocity was calculated using the following Hamilton (1980) method.

$$V_{oi} = v_r \cdot v_o, \quad v_o \text{ is the initial velocity for each sediment layer.}$$

Each layer thickness was determined by  $h = V_{oi} \cdot t$  where  $t$  is the sound speed through the sediment layer in one-way travel time. Compressional wave velocity was determined depending on the type of sediment by several equations.

$$V_p = v_o + 1.304 h - 0.741 h^2 + 0.257 h^3 \text{ for terrigenous sediment}$$

$$V_p = v_o + 1.713 h - 0.37 h^2 \text{ for calcareous sediment,}$$

$$V_p = v_o + 0.869 h - 0.267 h^2 \text{ for siliceous sediment.}$$

Interval velocity,  $V_p(l)$ , is the average velocity of the interval in the sediment between two reflectors. These values were taken from sonobuoy data (Fig. 1) (Ewing and Rabinowitz, 1984).

The shear wave velocity was calculated from the compressional wave value using the following relationships.

$$V_s = 3.884 V_p - 5.757 \text{ for } 1.521 < V_p < 1.555$$

$$V_s = 1.137 V_p - 1.485 \text{ for } 1.555 < V_p < 1.650$$

$$V_s = 0.991 - 1.36 V_p + 0.47 V_p^2 \text{ for } 1.650 < V_p < 2.150$$

$$V_s = 0.78 V_p - 0.962 \text{ for } V_p > 2.150$$

Attenuation  $K_p$  for compressional wave velocities were calculated using  $K_{po}$ , which is attenuation of compressional wave velocity versus mean grain sizes.

$$K_p = 0.214 - 0.0014 h - (0.214 \cdot (K_{po})) \times \text{Exp } h/200 \text{ for } K_{po} < 0.241 \text{ and } h < 450 \text{ m}$$

$$K_p = 0.214 \times (-0.00014h) \text{ for } K_{po} < 0.241 \text{ and } h > 450 \text{ m}$$

$$K_p = 0 \text{ for data greater than } 1000 \text{ m}$$

Density,  $\rho$ , was calculated using  $\rho = 1.135 V_p - 0.19$ .

\*These values were averaged over a layer.

\*\*These values were measured.

Table II. Geoacoustic model of site B.

| Sediment Type       | Depth (km) | $V_p$ (km/sec) | $V_p(l)$ (km/sec) | $V_s$ (km/sec) | $K_p$ (dB/m/kHz) | $\rho$ (g/cm <sup>3</sup> ) |
|---------------------|------------|----------------|-------------------|----------------|------------------|-----------------------------|
| Water               | 0.075      | 1.508          |                   |                |                  |                             |
| Fluvial Deposit     | 0.000      | 1.629          | 1.84              | 0.367          | 0.203            | 1.7                         |
|                     | 0.025      | 1.661          |                   | 0.401          | 0.201            | 1.7                         |
|                     | 0.050      | 1.692          |                   | 0.415          | 0.198            | 1.7                         |
|                     | 0.100      | 1.752          |                   | 0.444          | 0.193            | 1.8                         |
|                     | 0.200      | 1.862          |                   | 0.505          | 0.182            | 1.9                         |
|                     | 0.300      | 1.960          |                   | 0.570          | 0.170            | 2.0                         |
|                     | 0.400      | 2.048          |                   | 0.636          | 0.157            | 2.1                         |
|                     | 0.500      | 2.128          |                   | 0.702          | 0.146            | 2.2                         |
| $A^u$               | 0.600      | 2.200          |                   | 0.754          | 0.133            | 2.3                         |
| Shallow Water Marl  | 0.625      | 2.424          | 2.02              | 0.928          | 0.130            | 2.6                         |
|                     | 0.650      | 2.454          |                   | 0.952          | 0.126            | 2.6                         |
|                     | 0.675      | 2.485          |                   | 0.976          | 0.123            | 2.6                         |
|                     | 0.700      | 2.515          |                   | 1.000          | 0.120            | 2.7                         |
| Terrigenous Deposit | 0.750      | 2.228          | 2.51              | 0.776          | 0.114            | 2.3                         |
|                     | 0.800      | 2.259          |                   | 0.800          | 0.107            | 2.4                         |
|                     | 0.850      | 2.289          |                   | 0.823          | 0.101            | 2.4                         |
|                     | 0.900      | 2.319          |                   | 0.847          | 0.094            | 2.4                         |
|                     | 0.950      | 2.348          |                   | 0.870          | 0.088            | 2.5                         |
|                     | 1.000      | 2.378          |                   | 0.893          | 0.082            | 2.5                         |
|                     | 1.100      | 2.438          |                   | 0.940          |                  | 2.6                         |
|                     | 1.200      | 2.500          |                   | 0.988          |                  | 2.6                         |
| J                   | 1.303      | 2.568          |                   | 1.041          |                  | 2.7                         |
| Dolomitic Marl      | 1.350      | 3.150**        | 3.18              | 1.510**        |                  | 2.63**                      |
|                     | 1.453      |                |                   |                |                  |                             |
| Basement (Granite)  |            |                | 5.520             |                | 3.040**          | 2.67**                      |

Notes: Table II was calculated using the same equations and notes used for the model of site A. The bottom water velocity is 1508.23 m/sec at a water depth of 75 m. The basement in this site is granitic.

Table III. Geoacoustic model of site C.

| Sediment Type                 | Depth (km) | $V_p$ (km/sec) | $V_p(l)$ (km/sec) | $V_s$ (km/sec) | $K_p$ (dB/m/kHz) | $\rho$ (g/cm <sup>3</sup> ) |
|-------------------------------|------------|----------------|-------------------|----------------|------------------|-----------------------------|
| Water                         | 5.050      | 1.545          |                   |                |                  |                             |
| Calcareous Ooze               | 0.000      | 1.519          | 1.65              | 0.143          | 0.020            | 1.5                         |
|                               | 0.050      | 1.604          |                   | 0.338          | 0.056            | 1.6                         |
|                               | 0.100      | 1.687          |                   | 0.412          | 0.082            | 1.7                         |
|                               | 0.150      | 1.768          |                   | 0.451          | 0.101            | 1.8                         |
|                               | 0.175      | 1.807          |                   | 0.473          | 0.109            | 1.9                         |
|                               | 0.200      | 1.847          |                   | 0.496          | 0.115            | 1.9                         |
|                               | 0.205      | 1.855          |                   | 0.501          | 0.116            | 1.9                         |
|                               |            |                |                   |                |                  |                             |
| Siliceous Turbidite and Chert | 0.225      | 1.722          | 2.02              | 0.428          | 0.123            | 1.8                         |
|                               | 0.250      | 1.741          |                   | 0.438          | 0.126            | 1.8                         |
|                               | 0.275      | 1.759          |                   | 0.447          | 0.129            | 1.8                         |
|                               | 0.300      | 1.777          |                   | 0.456          | 0.131            | 1.8                         |
|                               | 0.325      | 1.794          |                   | 0.466          | 0.132            | 1.8                         |
|                               | 0.350      | 1.811          |                   | 0.475          | 0.133            | 1.9                         |
|                               | 0.398      | 1.843          |                   | 0.494          | 0.133            | 1.9                         |
| Carbonaceous Shale            | 0.400      | 2.176          | 1.96 – 2.263      | 0.736          | 0.134            | 2.3*                        |
|                               | 0.425      | 2.211          |                   | 0.763          | 0.134            |                             |
|                               | 0.450      | 2.246          |                   | 0.790          | 0.133            |                             |
|                               | 0.500      | 2.314          |                   | 0.843          | 0.146            |                             |
|                               | 0.525      | 2.347          |                   | 0.869          | 0.143            |                             |
|                               | 0.550      | 2.380          |                   | 0.894          | 0.139            |                             |
|                               | 0.592      | 2.433          |                   | 0.936          | 0.936            | 0.134                       |
|                               |            |                |                   |                |                  |                             |
| Oceanic Basement (Basalt)     |            | 5.300**        |                   | 2.680**        | 0.02**           | 2.7**                       |

Notes: Site C had a water depth of 5050 m and a bottom water velocity of 1545.10 m/sec. The same calculations apply as those used for site A. However, since the oceanic basement is shallower, attenuation was calculated throughout the layers, as were the shear and compressional wave velocities.



U230932